Reversible Formation of Ammonium Persulfate/Sulfuric Acid Graphite Intercalation Compounds and Their Peculiar Raman Spectra

Ayrat M. Dimiev,[†] Sergei M. Bachilo,[†] Riichiro Saito,[§,*] and James M. Tour[†,‡,*]

[†]Departments of Chemistry, [‡]Mechanical Engineering and Materials Science, and Computer Science, and the Smalley Institute for Nanoscale Science and Technology, Rice University, MS-222, 6100 Main Street, Houston, Texas 77005, United States, and [§]Department of Physics, Tohoku University, Sendai, 980-8578, Japan

ABSTRACT

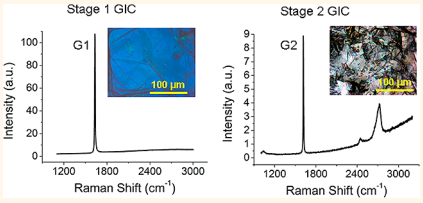

Graphite intercalation compounds (GICs) can be considered stacks of individual doped graphene layers. Here we demonstrate a reversible formation of sulfuric acid-based GICs using ammonium persulfate as the chemical oxidizing agent. No covalent chemical oxidation leading to the formation of graphite oxide occurs, which inevitably happens when other compounds such as potassium permanganate are used to charge carbon layers. The resulting acid/persulfate-induced stage-1 and stage-2 GICs are characterized by suppression of the 2D band in the Raman spectra and by unusually strong enhancement of the G band. The G band is selectively enhanced at different doping levels with different excitations. These observations are in line with recent reports for chemically doped and gate-modulated graphene and support newly proposed theories of Raman processes. At the same time GICs have some advantageous differences over graphene, which are demonstrated in this report. Our experimental observations, along with earlier reported data, suggest that at high doping levels the G band cannot be used as the reference peak for normalizing Raman spectra, which is a commonly used practice today. A Fermi energy shift of 1.20−1.25 eV and ∼1.0 eV was estimated for the stage-1 and stage-2 GICs, respectively, from the Raman and optical spectroscopy data.

KEYWORDS: graphite intercalation compounds · graphene · Raman spectroscopy · Fermi energy · enhancement

Graphite intercalation compounds (GICs) are produced by inserting different atomic, ionic, or molecular species (intercalants or intercalates) between the atomic layers of the host graphite. The resulting compounds possess unique properties that are not present in the parent materials. Thus GICs have been successfully tested for superconductivity and magnetism properties as well as in batteries and supercapacitors.[1−3] The number of graphene layers, *n*, sandwiched between the two intercalant layers is referred to as the stage number, and the corresponding GICs are called stage-*n* GICs.

Most GICs are unstable in air, which is also true for H_2SO_4-GICs. Unlike many other substances, H_2SO_4 does not spontaneously intercalate into graphite because the formation of a GIC from H_2SO_4 and graphite has a positive Gibbs free energy.[4] H_2SO_4-GIC can be produced only by means of electrochemical (anodic) or chemical oxidation reaction.[4−12] With electrochemical oxidation, the reaction is reversible since no C−O bonds are formed at low electrode potentials. However, the disadvantage of the electrochemical oxidation, compared to the chemical approach, is that it lacks conditions of reaction spontaneity, being fully controlled by electricity running through the circuit. With chemical oxidation, large-scale production of GICs can be readily carried out within minutes while being controlled only by the electrochemical potential of the oxidizing agent. On the other hand, the reactants normally used to charge the carbon layers (nitric acid and potassium permanganate)[11] inevitably lead to the irreversible oxidation of graphite by the formation of covalent C−O bonds; thus, graphite oxide is produced.

In this paper, we show that the stage-1 GIC is reversibly formed when graphite is exposed to an ammonium persulfate−sulfuric acid [$(NH_4)_2S_2O_8$−H_2SO_4] solution. The resulting GICs have several interesting features in their Raman spectra: the 2D band at ∼2700 cm^{-1} for the stage-1 and stage-2 GICs is suppressed while the G band is selectively enhanced. From the Raman and optical spectroscopy we

* Address correspondence to rsaito@flex.phys.tohoku.ac.jp; tour@rice.edu.

Received for review May 7, 2012 and accepted August 12, 2012.

Published online August 13, 2012
10.1021/nn3020147

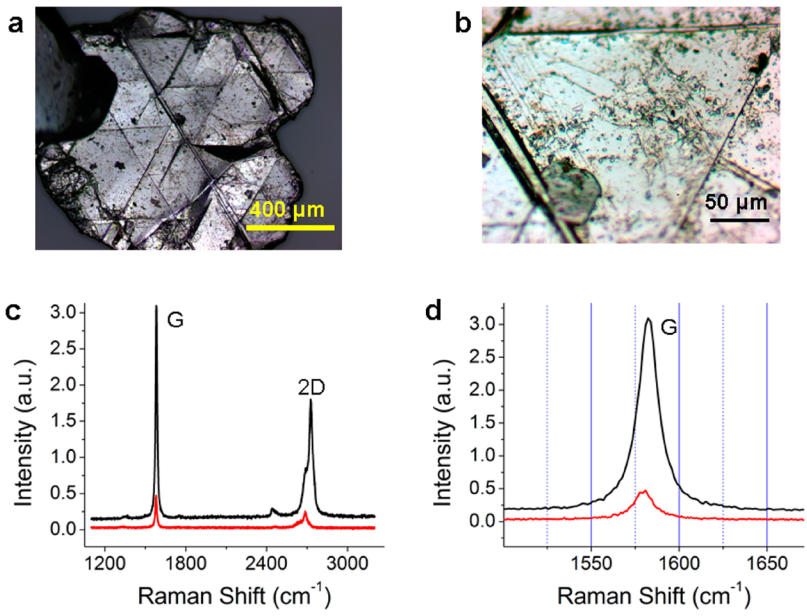

Figure 1. Photographs and Raman spectra from flake graphite. (a, b) Photographs of the FG at different magnifications. (c) Raman spectra from pristine FG taken with the two excitation lasers: 514 nm (black) and 633 nm (red). (d) Expansion of (c) at the G band.

estimated the Fermi energy shift for the stage-1 and stage-2 GICs.

RESULTS AND DISCUSSION

Flake Graphite and Stage-1 GIC. Flake graphite (FG) was used as the parent material. While Raman spectroscopy was the main experimental method used in this work to monitor the staging phenomena, the structure of as-prepared GICs was independently confirmed by XRD analysis (Figure S1). In the Raman spectra of the GICs, we observed the four distinct G-peak positions: 1587, 1607−1612, 1617−1622, and 1632−1634 cm^{-1}. The observed bands correspond to pristine graphite, higher stage $n > 2$, stage-2, and stage-1 GICs, respectively. We will refer to these peaks as G, G*n*, G2, and G1, respectively. The Raman spectra acquired with different excitations are normalized to the same laser power value. Thus the arbitrary intensity units serve as relative signal intensities.

The parent FG is metallic gray (Figure 1a), but it appears white at higher magnification (Figure 1b). The straight lines cross through the entire flake surface and intersect at 60° and 120° angles, which reflect the edges of graphite with high symmetry. The Raman spectrum (Figure 1c) is characterized by the G band at 1582 cm^{-1} and the 2D band at ∼2700 cm^{-1}. The spectrum also contains weak signals for the D band at 1350 cm^{-1} and G* band at 2450 cm^{-1}. The 2D band is highly dispersive as a function of the laser energy; its higher component appears at 2725 cm^{-1} with the 514 nm laser and at 2686 cm^{-1} with the 633 nm laser. The dispersion behavior of the 2D band is understood by the double resonance Raman effect.[13,14] The G band intensity of FG with the 514 nm laser is much larger than that with the 633 nm laser, and the ratio of the G band integral intensities is given by $G_{514}/G_{633} = 6.91$.

After treatment with the $(NH_4)_2S_2O_8-H_2SO_4$ solution, FG acquires a deep blue color (Figure 2a). The XRD data are consistent with the literature data[6,10] and clearly show the presence of the stage-1 GIC with a repeat distance I_c = 7.98 Å (Supporting Information, Section 1). The Raman spectra (Figure 2b, c) are characterized by a single G1 band at 1633 cm^{-1}. The G1 peak is blue-shifted relative to the G peak position of FG due to the charging of carbon layers by the acceptor-type intercalant and is consistent with the earlier reported data.[5] The G1 peak is intense with narrow spectral width. The full width at half-maximum (fwhm) of the peak is ∼11 cm^{-1} when the analysis is done using the 514 nm laser and ∼9 cm^{-1} when the analysis is done using the 633 nm laser. Note that the fwhm for pristine FG is ∼16 cm^{-1} when using either laser for the analysis. It should be mentioned that the G peak sharpening was previously explained by the nonadiabatic removal of the Kohn anomaly at the Γ point.[15,16] Classically, the G1 peak sharpening should be attributed to a more uniform structure of the stage-1 GIC within a laser spot compared with parent FG. The G1 band is selectively enhanced compared with the case of the pristine FG with the two different lasers. Thus with the 514 nm laser, the G peak intensity for stage-1 GIC is 28.7 times higher compared to that of the pristine FG ($G1_{514}/G_{514}$ = 28.7), while with the 633 nm laser the $G1_{633}/G_{633}$ ratio is 19.6. These are the numbers for the spectra presented in Figure 2. In different experiments the G band enhancement with the 514 nm laser varied from 28 to 33, so the value ∼30 can be considered as an average. There is no 2D band

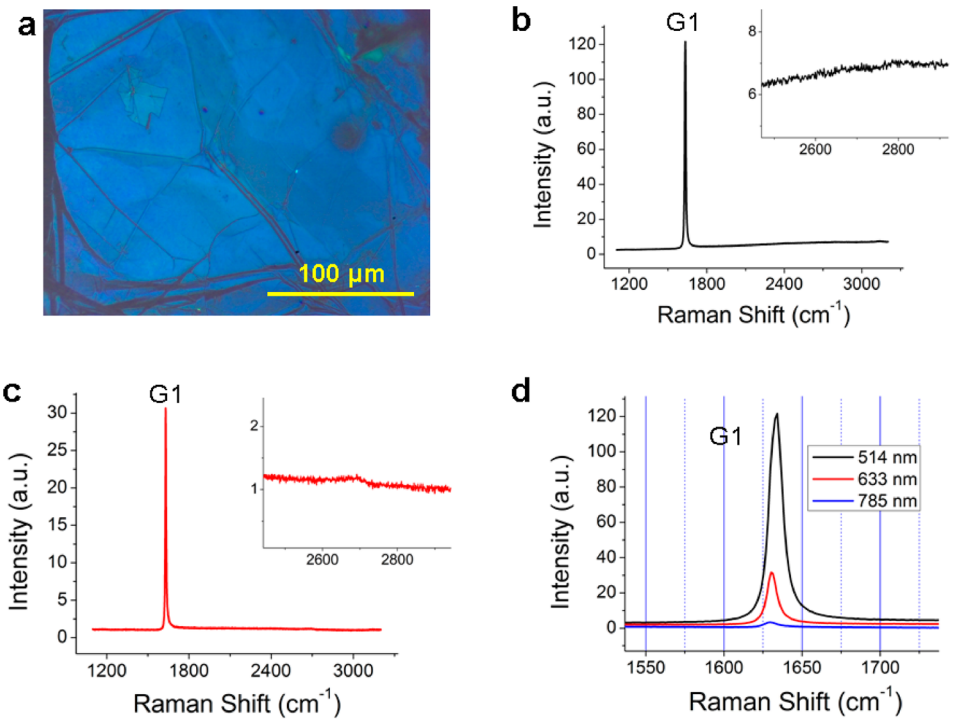

Figure 2. Characteristics of a stage-1 GIC. (a) Photograph of a stage-1 GIC. (b) Raman spectrum acquired using the 514 nm laser. The inset shows the expanded area near 2700 cm^{-1}. The 2D peak cannot be observed even though the intensity of the inset is magnified ~20× compared to the main spectrum. (c) Raman spectrum acquired using the 633 nm laser. The inset shows the area at ~2700 cm^{-1}. (d) G1 band relative intensities with the three different lasers.

in the spectra of the stage-1 GIC (Figure 2c), which is normally situated at ~2700 cm^{-1} for graphene or graphite. The baseline is flat in the analysis using the 514 nm laser and only slightly curved in the analysis using the 633 nm laser (Figure 2b, c).

Reversibility of the $(NH_4)_2S_2O_8$–H_2SO_4-Induced Intercalation. Quenching and washing the as-prepared stage-1 GIC with water converts the GIC back to the original graphite. There are indications, however, that some amount of sulfuric acid remains trapped between the graphite layers, forming residual GIC. It takes a few hours to convert FG to the stage-1 GIC. In this experiment, we kept our sample in $(NH_4)_2S_2O_8$–H_2SO_4 solution for 7 days. Next, the resulting stage-1 GIC was washed with copious amounts of water, accompanied by stirring and sonication, until the pH of the wash water was neutral. We will refer to the sample subjected to one intercalation–deintercalation cycle as the I-D sample. The XPS analysis of the I-D sample shows the presence of 8 atom % oxygen. Part of this oxygen signal comes from the oxygen sorbed on the graphite surface; all graphite samples show some oxygen content in their XPS spectra. The C1s XPS spectrum (Figure 3a) of the I-D sample contains a small peak at 286.6 eV, in addition to the main carbon peak at 284.4 eV. The signal at 286.6 eV can come from two independent sources: (a) the carbon layers adjacent to residual sulfuric acid trapped between the layers and (b) the carbon atoms covalently bonded to oxygen. In either case, the content of this type of carbon is very low and otherwise the spectrum is identical to that of intact graphite. The thermogravimetric analysis (TGA) data (Figure 3b) do not show any weight loss in the 160 to 180 °C range, where the graphite oxide normally loses its oxygen functional groups,[16] suggesting that little graphite oxide is present in the sample. The measured weight loss is 1.0% in the 218 to 262 °C interval and 5.5% in the 332 to 504 °C interval, above the boiling point of H_2SO_4. The high-temperature weight loss suggests decomposition of a residual GIC.

The Raman spectra taken from 9 out of 10 spots on the I-D sample are identical to the spectrum of the FG. One out of 10 spots indicates the presence of a high-stage GIC phase, which is consistent with the presence of a residual GIC. The most notable difference between the I-D sample and the control sample is found in the XRD data (Figure 3c, d): the 002 peak at an angle $2\theta = 26.1°$ is broadened and slightly shifted toward smaller 2θ values compared with the control sample. The corresponding interlayer distance is 0.341 nm, which is slightly larger than 0.335 nm for graphite, and the crystallite thickness, L_c, is estimated as 6.62 nm by the XRD spectral width. This is consistent with formation of expanded or turbostratic graphite. Note that the XRD data show the change in the graphite morphology, not in the chemical structure of the graphene layers that remain intact. Also, there is a very weak signal at $2\theta = 11.6°$, which likely corresponds to graphite oxide. Overall, the I-D sample appears as normal graphite: it is gray, possesses luster, and is very soft and malleable.

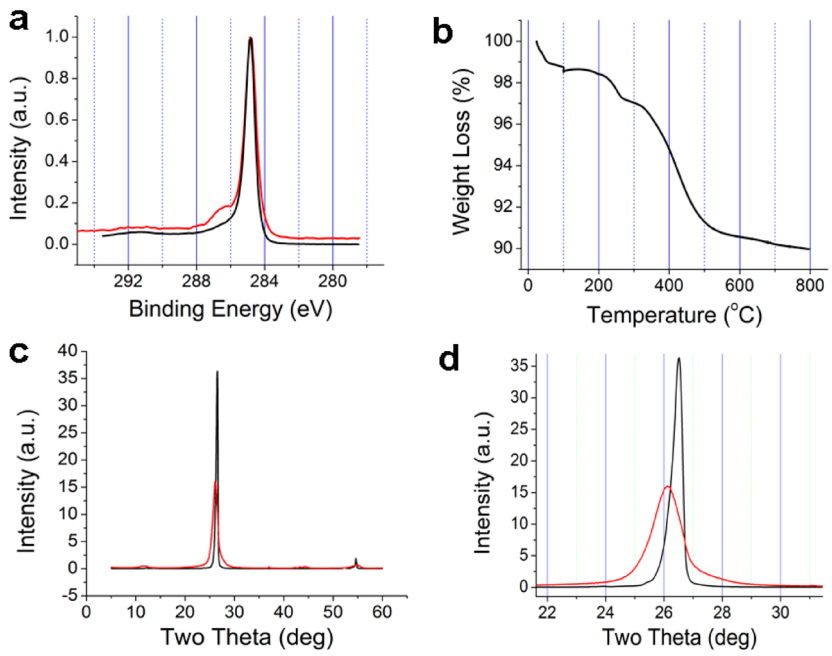

Figure 3. Characteristics of the graphite sample subjected to one intercalation−deintercalation cycle. (a) C1s XPS spectra for the I-D sample (red line) and original graphite (black line). (b) Weight loss of the I-D sample. (c) XRD data for the I-D sample (red line) *vs* control sample (black line). (d) An expansion of (c) around 26 deg.

The content of graphite oxide is very low. Considering the time that the graphite was exposed to the $(NH_4)_2S_2O_8-H_2SO_4$ mixture (7 days at room temperature), this degree of oxidation is negligible. As a reference, exposing graphite to potassium permanganate or potassium chlorate in sulfuric acid for the same period of time[17,18] results in substantial oxidation of the graphite and formation of graphite oxide. Thus we concluded that ammonium persulfate enables a nearly complete reversible formation of GICs without destroying the host carbon layers.

Stage-2 and Mixed Stage GICs. Upon standing in air, the stage-1 GIC gradually changes in color from blue to grayish-white (Figure 4a), manifesting transition of the stage-1 GIC to a stage-2 GIC due to deitercalation. Under ambient conditions, this transition occurs in a matter of 1−3 min, and higher stage numbers are formed. By sealing the GIC flake between a microscope slide and a coverslip, we control the rate of transition and can stop it at the stage-2 conditions sufficiently long for sample characterization. The Raman spectrum changes accordingly (Figure 4b−d). The 2D peak for the stage-2 GIC now appears at ~2700 cm^{-1} on the spectrum taken using the 514 nm laser (Figure 4b). The 2D peak is not single Lorentzian and can be deconvoluted with the four peaks (see SI for details), suggesting AB stacking of two adjacent carbon layers after deintercalation.[19] This ability of graphene layers to be restacked in AB order during the stage-1−stage-2 transition is interesting. Note that the 2D peak is still missing on the spectrum acquired using the 633 nm laser (Figure 4c).

The G2 peak red-shifts compared to the G1 peak, and the G2 spectral position is at 1620 cm^{-1} with 514 nm excitation and at 1617 cm^{-1} with 633 nm excitation This observation is consistent with formation of stage-2 GIC, which is confirmed by XRD data (Supporting Information, Section 1). For a stage-2 GIC, each carbon layer is bound to the intercalant on one side and to another carbon layer on the other side. Thus the transferred charge on the carbon layer is lower compared to the stage-1 GIC, where every carbon layer is situated between two intercalant layers. The G2 peak is still enhanced compared to the G peak of pristine graphite, but it is more significantly enhanced with the 633 nm laser compared to the 514 nm laser. The G2 enhancement by the two different lasers for the stage-2 GIC is opposite that found for the stage-1 GIC. Thus $G2_{633}/G_{633} = 24.1$, while $G2_{514}/G_{514} = 1.90$.

The laser-selective enhancement of the G band is especially representative with the mixed stage samples, where two different phases are present at the same acquisition spot. To prepare the mixed stage samples, the $(NH_4)_2S_2O_8-H_2SO_4$ solution, at a stage-1 GIC, was diluted with water [17:1 $(NH_4)_2S_2O_8-H_2SO_4$ solution:water], which facilitates partial deintercalation. The mixed stage areas have bright intense colors as observed under an optical microscope (Figure 5a). The new color appears when the intercalant is removed from a specific number of graphite galleries.

The spot color can serve as an indication of the degree of deintercalaton. The content of stage-1 *vs* stage-2 phases decreases as tinges of red and neutral to white colors are added to the original deep-blue color. Thus the spectrum acquired from the violet-colored spot (blue with a little red) using the 514 nm laser (Figure 5b) contains the G1 component only.

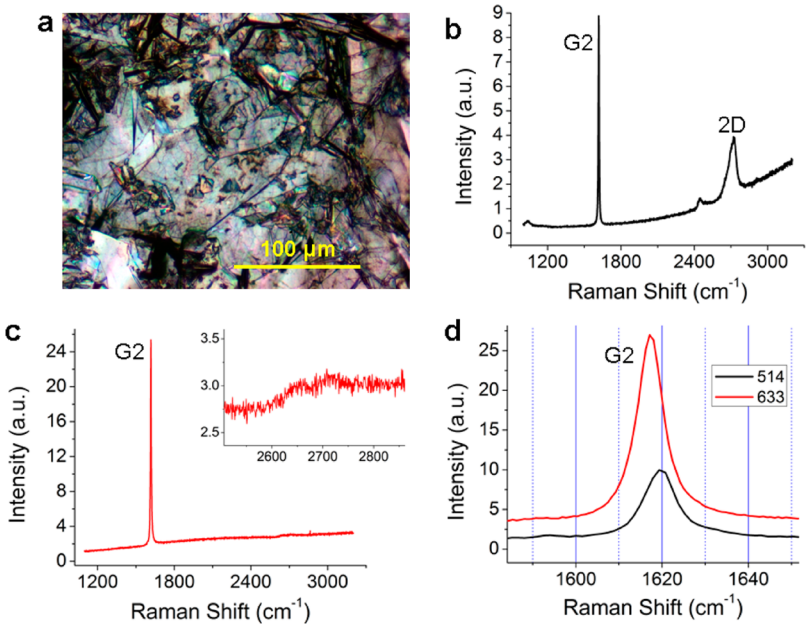

Figure 4. Characteristics of a stage-2 GIC. (a) Photograph of a stage-2 GIC. (b) Raman spectra acquired with the 514 nm laser. (c) Raman spectra acquired with the 633 nm laser. The inset shows the area ~2700 cm^{-1}, where the 2D peak normally appears. The *y*-scale is magnified ~10× compared with the main spectrum. (d) G2 peak area from the spectra acquired using the two different lasers. The 3 cm^{-1} difference in the G2 peak positions for the two lasers is related to calibration.

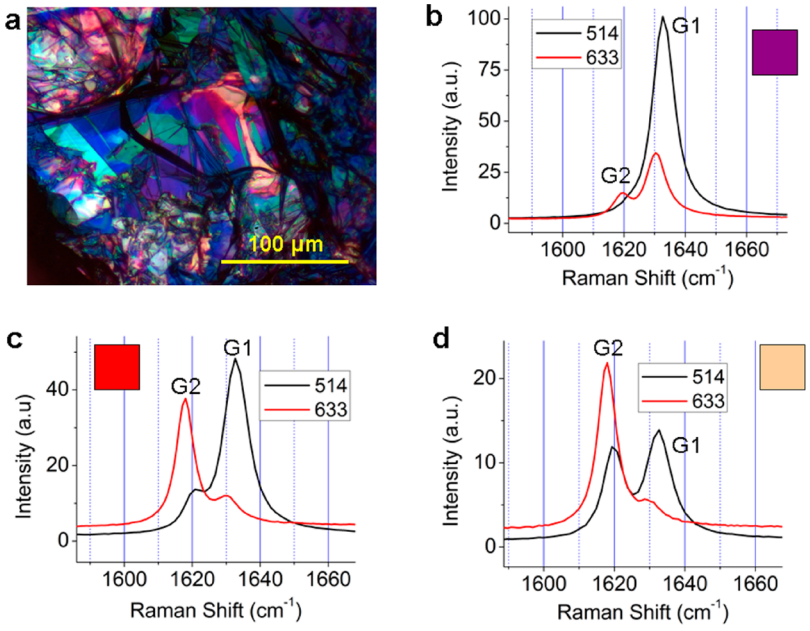

Figure 5. Partially deintercalated stage-1 GIC. (a) Photograph of the partially deintercalated stage-1 GIC. The brightly colored areas are the mixed stage GIC. (b) Raman spectra taken from the violet and purple-colored spots. (c) Raman spectra taken from the red-colored spots. (d) Raman spectra taken from the neutral ivory-colored spots.

The spectrum suggests the presence of a pure stage-1 GIC. However, the spectrum taken from the same spot using the 633 nm laser clearly shows the G2 component. The spectrum taken from the red spot (Figure 5c) shows the mixed stage GICs. Note that the G1 peak dominates the spectrum taken using the 514 nm laser, while the G2 peak dominates the spectrum taken using the 633 nm laser. The ivory-colored spots are characterized with an even lower G1/G2 ratio (Figure 5d). Both the G2 and G1 intensities decrease as the content of stage-2 phase increases. This most likely occurs due to the decrease of the probing depth with deintercalation. The advantage of the data acquired from the mixed stage area is that the spectra contain both peaks G1 and G2 on the same excitation profile, and the selective enhancement of the two

bands with the two lasers is apparent. The observed selective G band enhancement is very important. As was pointed out by Basco,[20] the G-band intensity "is often assumed to remain constant under the change of many external parameters", and it is therefore used as a reference peak upon which to normalize spectra.[21−23] At least for significant doping levels, such a convention in normalization will lead to misasignments.

Discussion of G-Band Selective Enhancement and the 2D-Band Suppression. One of the earliest reports of laser-selective G peak enhancement for the electrochemically prepared H_2SO_4-GICs was by Eklund *et al.*[24] Eklund *et al.* explained the observed phenomenon by the resonance for incident photon energies in the region close to the threshold values for electronic interband absorption. Recently strong enhancement of the G band at threshold energy values for the doped graphene was shown theoretically by Basko.[20] Suppression of the 2D band, on the other hand, was experimentally demonstrated for chemically doped single- and few-layer graphene.[22,25] Finally, experimental data similar to that observed in this work was reported recently for the gate-modulated single-layer graphene:[26,27] the G band was enhanced, while simultaneously the 2D band was suppressed. While the 2D band suppression can indeed be explained by the Pauli blocking effect, as was suggested by Zhao *et al.*,[22] simultaneous G band enhancement is difficult to envision within the same theory. Basco[20] has shown that for undoped graphene, the experimental G band intensity is lower than is theoretically predicted due to destructive interference. Chen *et al.*[27] explained the G band enhancement phenomenon with doping by elimination of destructive interference at laser energies in the vicinity of the double Fermi energy (E_f). Thus, G band enhancement permits one to estimate the Fermi energy shift (E_f) as half of the incident laser energy, which provides the highest enhancement. Since for our stage-1 GIC the strongest G-band enhancement is observed with the 514 nm laser, we can estimate the Fermi shift as half of the 514 nm laser energy; hence $\approx$ 1.2 eV. Similarly, for the stage-2 GIC, the E_f can be estimated as half of the 633 nm laser energy, thus being ~1.0 eV.

The pathways leading to the 2D mode, on the other hand, always interfere constructively;[27] thus blocking part of the pathways leads to decreased Raman intensity. Our experimental data additionally support the proposed suppression−enhancement mechanism. According to Chen *et al.*,[27] the higher the doping level, the more pathways should be blocked and the more destructive interference is eliminated, resulting in stronger G band intensity. This is exactly what we observe in our experiments. For the stage-1 GIC ($E_f \approx$ 1.2 eV) with the 514 nm laser, the G1 peak is enhanced ~30 times compared to parent graphite. For the stage-2 GIC ($E_f \approx$ 1.0 eV) with the 633 nm laser, the G2 peak is enhanced ~24 times.

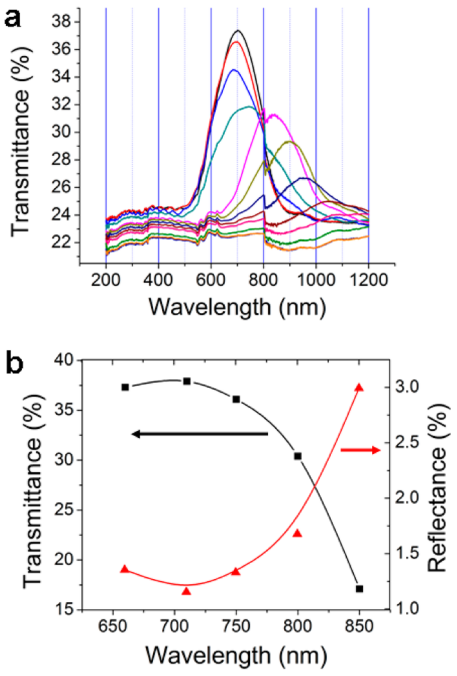

Figure 6. Optical characteristics of H_2SO_4-GICs. (a) Change in transmittance of stage-1 H_2SO_4-GIC associated with its transition to stage-2 GIC. Continuous spectra were acquired from a film of overlapping flakes. Data are represented as the percent from the incident light. The transmittance maximum gradually shifts from 700 nm for the stage-1 GIC to 950 nm for the stage-2 GIC and toward lower energies for higher stage GICs. (b) Transmittance and reflectance values simultaneously acquired from a single flake of stage-1 GIC. Discrete wavelengths were generated by a laser as the source of the incident light. The data are represented as the percent from the incident light.

The main difference between our data and that reported on gate-modulated graphene[26,27] is the significantly stronger G band enhancement overall (~30 in our experiments *vs* 3.5 in ref 27). In part we attribute this difference to the difference between our samples: multilayer GIC *vs* substrate-supported single-layer graphene. Intercalation increases the graphite transparency in the visible light region, which in turn increases the probing depth; it is known that the G band intensity is proportional to the number of graphene layers probed. We do not know, however, if sample transparency can be solely accountable for such a high difference in the G band enhancement.

Optical Spectroscopy. The Fermi shift in GICs can also be determined from optical measurements.[28−30] Both stage-1 and stage-2 H_2SO_4-GICs have transmission windows at certain wavelength values, which is relevant to the Fermi energy. For electrochemically prepared stage-1 H_2SO_4-GIC, the number of carbon atoms (p) per one electron transferred from graphite to acceptor varies from 21 to 28 (p = 21−28).[9,24,28−30] The experimental optical data reported for electrochemically prepared stage-1 H_2SO_4-GICs have some variance. Henning[31] reported a transmission maximum at 680 nm. Zhang *et al.*[30] reported reflectance minimums

at ~653 and ~776 nm for p = 21 and p = 28, respectively. We measured the optical properties of our GICs using two different techniques, and the data are reported in Figure 6. First we performed the *in situ* measurements of the stage-1 GIC during its transition to the stage-2 GIC (Figure 6a). The stage-1 GIC has a well-pronounced transmittance maximum at 700 nm. The spectral width of the transmission window is ~200 nm. As the stage-1 GIC transforms to a stage-2 GIC, the transmission decreases and its maximum shifts toward lower energies. This observation is consistent with decreasing the probing depth and lowering the Raman signal intensity with deintercalation (Figure 5). In a different experiment we simultaneously measured transmittance and reflectance for the same stage-1 GIC flake (Figure 6b). Surprisingly, our samples showed very low reflectance (<2% of incident light) within the transmission window; thus any change in transmittance is related to absorbance. Nevertheless, the transmittance maximum and reflectance minimum (Figure 6b) coincide well at ~700 nm, and this is in good agreement with the data acquired with the continuous source of light (Figure 6a). By comparing this wavelength with the data obtained by Zhang *et al.*,[30] the number of carbon atoms bearing one elemental charge can be estimated as $p \approx 24$. The corresponding Fermi shift (calculated as in refs 24, 28–30) is 1.25 eV. This value is in good agreement with those obtained from the Raman spectra. Thus, on the basis of different experimental techniques, we estimate the Fermi shift in our chemically derived stage-1 H_2SO_4-GIC as 1.20–1.25 eV.

CONCLUSION

A new H_2SO_4-based GIC was prepared using ammonium persulfate to assist in the intercalation. The formation of GICs is reversible; no chemical oxidation of graphite occurs. The resulting GICs are characterized by a suppressed 2D band in the Raman spectra due to Pauli blocking. The G peak signal is selectively enhanced by the 514 nm and the 633 nm lasers due to elimination of destructive interference and due to increasing of the probing depth in the GICs. This observation argues against using the G band as the reference peak for normalizing Raman spectra for high doping levels, even though such normalization is often performed. The Fermi energy shift for the stage-1 GIC was estimated independently from different experimental data to be ~1.20–1.25 eV and ~1.0 eV for stage-1 and stage-2 samples, respectively. With Raman spectroscopy becoming the overriding tool in graphene structure delineation, continued characterization details can be critical to solving key questions of graphitic structures.

METHODS

To prepare the GIC, $(NH_4)_2S_2O_8$ (1.0 g) was added to 98% H_2SO_4 (10.0 mL) with constant swirling. The mixing was accompanied by gas evolution from the partial decomposition of the persulfate anion. After 5 min, graphite (0.2–0.4 g) was added to the solution and swirling was continued. The formation of the GIC was indicated by the appearance of the deep blue color of the graphite. Complete intercalation was achieved in 6–8 h. The graphite starting material used was flake graphite from Sigma-Aldrich, batch # 13802EH.

Optical micrographs were acquired using a Zeiss Axioplan 2, equipped with AxioCam MRc. The reflected mode was used with a white incandescent light source. Two types of lenses were used: Zeiss Epiplan 10×, 0.2 for low-magnification imaging, and Zeiss LD Epiplan 20×, 0.4 HD DIC for higher magnification. The Raman spectra were acquired using a Renishaw Raman RE01 microscope with 40× lens. Wavelength lasers of 514 and 633 nm were used for excitation. X-ray powder diffraction was obtained using a Rigaku D/Max 2550 diffractometer with Cu Kα radiation (λ = 1.5418 Å). The data were analyzed and processed using the Jade 9 software package. TGA was performed with a TA Instruments Q50; nitrogen was used as balance purge gas, and argon was used as sample purge gas. A heating rate of 10 °C/min was used.

Conflict of Interest: The authors declare no competing financial interest.

Acknowledgment. A.D. and J.M.T. acknowledge the ONR (#00006766, N00014-09-1-1066) and the AFOSR (FA9550-12-1-0035, FA9550-09-1-0581). R.S. acknowledges a MEXT grant (No. 20241023).

Supporting Information Available: (1) X-ray diffraction data, (2) Raman spectra acquired with a 488 nm laser, (3) Raman laser power dependence data, and (4) deconvolution of the 2D peak in Raman spectra of stage-2 GIC acquired with the 514 nm laser. This material is available free of charge *via* the Internet at http://pubs.acs.org.

REFERENCES AND NOTES

1. Dresselhaus, M. S.; Dresselhaus, G. Intercalation Compounds of Graphite. *Adv. Phys.* **2002**, *51*, 1–186.
2. Zabel, H; Solin, S. A. *Graphite Intercalation Compounds*, Vol.1; Springer-Verlag: Berlin, New York, 1990.
3. Enoki, T.; Endo, M. *Graphite Intercalation Compounds and Applications*; Oxford University Press: USA, 2003.
4. Aronson, S.; Frishberg, C.; Frankl, G. Thermodynamic Properties of the Graphite-Bisulfate Lamellar Compounds. *Carbon* **1971**, *9*, 715–723.
5. Eklund, P. C.; Olk, C. H.; Holler, F. G.; Spolar, J. G.; Arakawa, E. T. Raman Scattering Study of the Staging Kinetics in the C-Face Skin of Pyrolytic Graphite- H_2SO_4. *J. Mater. Res.* **1986**, *1*, 361–367.
6. Yosida, Y.; Tanuma, S. *In Situ* Observation of X-Ray Diffraction in a Synthesis of H_2SO_4-GICS. *Synth. Met.* **1989**, *34*, 341–346.
7. Nishitani, R.; Sasaki, Y.; Nishina, Y. Kinetics of Staging Transition in H_2SO_4-Graphite Intercalation Compounds. *Synth. Met.* **1989**, *34*, 315–321.
8. Metrot, A.; Fischer, J. E. Charge Transfer Reactions during Anodic Oxidation of Graphite in H_2SO_4. *Synth. Met.* **1981**, *3*, 201–207.
9. Besenhard, J. O.; Wudy, E.; Möhwald, H.; Nickl, J.; Biberacher, W.; Foag, W. Anodic Oxidation of Graphite in H_2SO_4. Dilatometry–*In Situ* X-Ray Diffraction–Impedance Spectroscopy. *Synth. Met.* **1983**, *7*, 185–192.
10. Inagaki, M.; Iwashita, N.; Kouno, E. Potential Change with Intercalation of Sulfuric Acid into Graphite by Chemical Oxidation. *Carbon* **1990**, *28*, 49–55.

11. Moissette, A.; Fuzellier, H.; Burneau, A.; Bubessy, J.; Lelaurain, M. Sulfate Graphite Intercalation Compounds: New Electrochemical Data and Spontaneous Intercalation. *Carbon* **1995**, *33*, 123–128.
12. Shioyama, H.; Fujii, R. Electrochemical Reactions of Stage 1 Sulfuric Acid−Graphite Intercalation Compound. *Carbon* **1987**, *25*, 771–774.
13. Saito, R.; Gruneis, A.; Samsonidze, G. G.; Brar, V. W.; Dresselhaus, G.; Dresselhaus, M. S.; Jorio, A.; Cancado, L. G.; Fantini, C.; Pimenta, M. A.; *et al*. Double Resonance Raman Spectroscopy of Single-Wall Carbon Nanotubes. *New J. Phys.* **2003**, *5*, 157.
14. Jorio, A.; Dresselhaus, M.; Saito, R.; Dresselhaus, G. *Raman Spectroscopy in Graphene Related Systems*; Wiley-VCH Verlag GmbH and Co. KGaA: Weinheim, 2011.
15. Lazzeri, M.; Mauri, F. Nonadiabatic Kohn Anomaly in a Doped Graphene Monolayer. *Phys. Rev. Lett.* **2006**, *97*, 266407.
16. Pisana, S.; Lazzeri, M.; Casiraghi, C.; Novoselov, K. S.; Geim, A. K.; Ferrari, A. C.; Mauri, F. Breakdown of the Adiabatic Bork-Oppenheimer Approximation in Graphene. *Nat. Mater.* **2007**, *6*, 198–201.
17. Dimiev, A.; Kosynkin, D. V.; Alemany, L. B.; Chaguine, P.; Tour, J. M. Pristine Graphite Oxide. *J. Am. Chem. Soc.* **2012**, *134*, 2815–2822.
18. Szabo, T.; Berkesi, O.; Forgo, P.; Josepovits, K.; Sanakis, Y.; Petridis, D.; Dekany, I. Evolution of Surface Functional Groups in a Series of Progressively Oxidized Graphite Oxides. *Chem. Mater.* **2006**, *18*, 2740–2749.
19. Ferrari, A. C.; Meyer, J. C.; Scardaci, V.; Casiraghi, C.; Lazzeri, M.; Mauri, F.; Piscanec, S.; Jiang, D.; Novoselov, K. S.; Roth, S.; *et al*. Raman Spectrum of Graphene and Graphene Layers. *Phys. Rev. Lett.* **2006**, *97*, 187401–4.
20. Basko, D. M. Calculation of the Raman G Peak Intensity in Monolayer Graphene: Role of Ward Identities. *New J. Phys.* **2009**, *11*, 095011–12.
21. Basko, D. M.; Piscanec, S.; Ferrari, A. C. Electron-Electron Interactions and Doping Dependence of the Two-Phonon Raman Intensity in Graphene. *Phys. Rev. B* **2009**, *80*, 165413–10.
22. Zhao, W.; Tan, H. T.; Liu, J.; Ferrari, A. C. Intercalation of Few-Layer Graphite Flakes with $FeCl_3$: Raman Determination of Fermi Level, Layer by Layer Decoupling, and Stability. *J. Am. Chem. Soc.* **2011**, *133*, 5941–5946.
23. Elias, D. C.; Nair, R. R.; Mohiuddin, T. M. G.; Morozov, S. V.; Blake, P.; Halsall, M. P.; Ferrari, A. C.; Boukhvalov, D. W.; Katsnelson, M. I.; Geim, A. K.; *et al*. Control of Graphene's Properties by Reversible Hydrogenation: Evidence for Graphane. *Science* **2009**, *323*, 610–613.
24. Eklund, P. C.; Mahan, G. D.; Spolar, J. G.; Zhang, J. M.; Arakawa, E. T.; Hoffman, D. M. Resonant Raman Scattering in Metals at the Interband Absorption Threshold. *Phys. Rev. B* **1988**, *37*, 691–698.
25. Jung, N.; Kim, N.; Jockusch, S.; Turro, N. J.; Kim, P.; Brus, L. Charge Transfer Chemical Doping of Few Layer Graphenes: Charge Distribution and Band Gap Formation. *Nano Lett.* **2009**, *9*, 4133–4137.
26. Kalback, M.; Reina-Cecco, A.; Farhat, H.; Kong, J.; Kavan, L.; Dresselahaus, M. S. The Influence of Strong Electron and Hole Doping on the Raman Intensity of Chemical Vapor-Deposition Graphene. *ACS Nano* **2010**, *4*, 6055–6063.
27. Chen, C.-F.; Park, C.-H.; Boudouris, B. W.; Horng, J.; Geng, B.; Girit, C.; Zettl, A.; Crommie, M. F.; Segalman, R. A.; Louie, S. G.; *et al*. Controlling Inelastic Light Scattering Quantum Pathways in Graphene. *Nature* **2011**, *471*, 617–620.
28. Rigaux, C. In *Intercalation in Layered Materials*; Dresselhaus, M. S., Ed.; Plenum: New York, 1987.
29. Jean, M. S.; Menant, M.; Hau, N. H.; Rigaux, C.; Metrot, A. *In Situ* Optical Study of H_2SO_4-Graphite Intercalation Compounds. *Synth. Met.* **1983**, *8*, 189–193.
30. Zhang, J. M.; Hoffman, D. M.; Eklund, P. C. Optical Study of the *K*-Point Dispersion in Graphite- H_2SO_4. *Phys. Rev. B* **1986**, *34*, 4316–4322.
31. Henning, G. R. Optical Transmission of Graphite Compounds. *J. Chem. Phys.* **1965**, *43*, 1201–1206.